Contributions to Geophysics and Geodesy Vol. 39/4, 2009 (301–323)

Geothermal refraction problem for a 2-D body of polygonal cross-section buried in the two-layered earth

Milan HVOŽDARA[1], Dušan MAJCIN[1]

[1] Geophysical Institute of Slovak Academy of Sciences, Dúbravská cesta 9, Slovak Republic; e-mail: geofhvoz@savba.sk

Abstract: We present the exact boundary integral formulae for calculation of the geothermal anomaly due to a two dimensional body whose thermal conductivity is λ_T and its cross-section is bounded by the closed general polygonal contour. This body is buried in the superficial layer of conductivity λ_1. The half-space $z > h$ with the thermal conductivity λ_2 is considered as a substratum of models. The boundary integral technique for the solution of this problem requires the application of logarithmic potential terms in infinite series. Numerical calculations based on derived formulae revealed that the surface anomaly heat flow reflects the "topography" mainly of the upper boundary of the perturbing body. The derived algorithm and the developed numerical program enable calculations for a number of interesting models: intrusions, protrusions of the substratum etc.

Key words: geothermal models, boundary integral technique, geothermal measurements, heat flow refraction

1. Formulation and the B.I.E. solution

The solution of the forward geothermal refraction problems for two or three dimensional isolated bodies belongs to the "classical geophysics", e.g. *(Lebedev et al., 1955; Ljubimova et al., 1983)*. The exact analytical solutions by means of separation of variables in Laplace's or Poisson's equations was performed for "smooth bodies" such as sphere, cylinder, ellipsoid, using separability of these partial differential equations *(Moon and Spencer, 1971)*. The exact solution for polyhedral bodies can be performed using methods of finite differences, finite elements or boundary equations method. The last method mentioned seems to be more effective in comparison to the previous two, since numerical calculations are concentrated mainly to the boundary surface of disturbing body, see e.g. *(Chen and Beck, 1991)*.

The theory of the boundary integral calculations of geothermal anomalies due to 3D bodies bounded by a piecewise smooth (Lyapunov's) surface S and situated in two-layered earth was presented in the earlier paper *(Hvoždara and Valkovič, 1999)*. We generalize the presented 3D analysis to more complicated polygonal 2D body of thermal conductivity λ_T, bounded by the polygon L and buried in the superficial layer "1" $0 \le z \le h$ with the thermal conductivity λ_1. In this paper we suppose that the 2D body is bounded by the closed polygon with $N+1$ vertices in the plane (x, z), see Fig. 1. The vertices are denoted as $A_k, k = 1, 2, \ldots, N+1$, where $N \ge 3$,

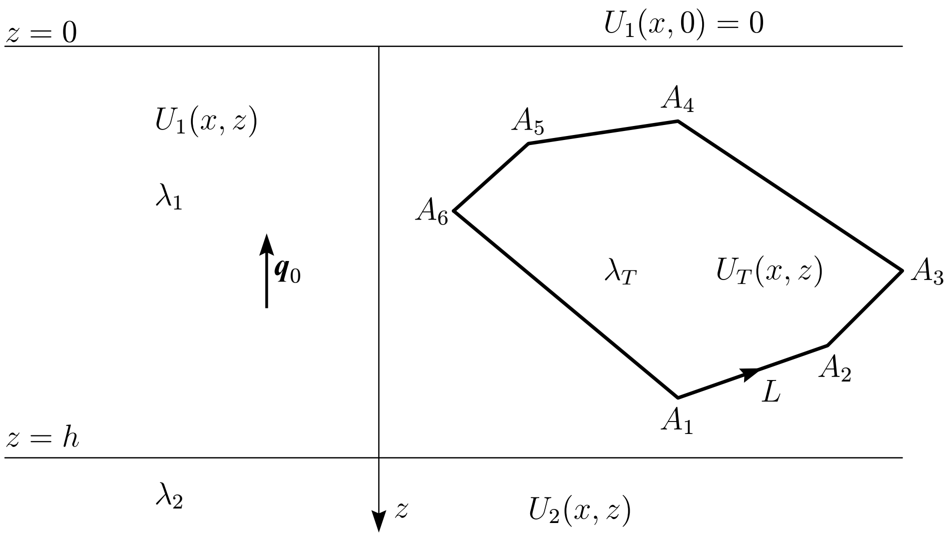

Fig. 1. Scheme for the two-dimensional perturbing body embedded in the first layer with uniform ambient geothermal heat-flow field density q_0.

and the first vertex A_1 is identical with the last one $A_{N+1} \equiv A_1$. These vertices are connected by the line segments T_k, their number is N and the lengths are T_k:

$$T_k = \left[(x_{k+1} - x_k)^2 + (z_{k+1} - z_k)^2\right]^{1/2} . \quad (1)$$

The theory of steady thermal field *(Carslaw and Jaeger, 1959)* enables us to calculate the temperature field $U(x, z)$ which obeys the Laplace equation

$\nabla^2 U(x, z) = 0.$

The density of the heat flow is

$\boldsymbol{q} = -\lambda \, \mathrm{grad} \, U.$

The unperturbed temperature field V_1 in the upper layer is given as a linear function of z:

$$V_1(x, z) = z(q_0/\lambda_1), \tag{2}$$

where q_0 is the unperturbed vertical heat flow density at the surface $z = 0$. Its analytical continuation into region "2" is

$$V_2(x, z) = z(q_0/\lambda_2) + (q_0 h/\lambda_1)(1 - \lambda_1/\lambda_2). \tag{3}$$

Since the physical properties of our model as well as the exciting thermal field are independent of y, we can use the well-known 2D boundary element apparatus for the solution. The transition from 3D problem to 2D one was discussed in detail in e.g. *(Hvoždara, 1983; Hvoždara and Schlosser, 1985)*. In our 2D model we consider the y-axis as a strike line of the perturbing body, so we can use the 2D analogs of the 3D Green's functions. It results in the following changes:

- the principal term $\left[(x - x')^2 + (y - y')^2 + (z - z')^2\right]^{-1/2}$ must be replaced by $\ln\left[(x - x')^2 + (z - z')^2\right]^{-1/2}$,
- similar changes must be done also in all terms of the infinite series obtained in the 3D Green's function used in the papers *(Hvoždara and Valkovič, 1999; Hvoždara, 2008)*,
- integration over the boundary surface S using the elements $\mathrm{d}\,S_Q$ of perturbing body must be replaced by the integration along the contour line L using the elements $\mathrm{d}\,\ell'$,
- the factor $1/(4\pi)$ should be replaced by $1/(2\pi)$.

Then the transformation of our 3D treatment given in *Hvoždara and Valkovič (1999)* for the case of polygonal 2D perturbing body now leads to the following formulae for temperatures in three media:

$$U_1(\boldsymbol{r}) = V_1(\boldsymbol{r}) + \frac{1}{2\pi}\int\limits_L f(\boldsymbol{r}')\frac{\partial}{\partial n'}\,g_1(\boldsymbol{r},\boldsymbol{r}')\,\mathrm{d}\,\ell', \tag{4a}$$

for $P(\boldsymbol{r}) \in \mathrm{Ext}(L)$ and $z \in \langle 0, h\rangle$. In the interior of 2D body the temperature is given by

$$U_T(\boldsymbol{r}) = \frac{\lambda_1}{\lambda_T}\left\{V_1(\boldsymbol{r}) - v_0 + \frac{1}{2\pi}\int\limits_L f(\boldsymbol{r}')\frac{\partial}{\partial n'}\,g_1(\boldsymbol{r},\boldsymbol{r}')\,\mathrm{d}\,\ell'\right\} +$$

$$+ (1 - \lambda_1/\lambda_T)v_0, \qquad P(\boldsymbol{r}) \in \mathrm{Int}(L), \tag{4b}$$

$$U_2(\boldsymbol{r}) = V_2(\boldsymbol{r}) + \frac{1}{2\pi}\int\limits_L f(\boldsymbol{r}')\frac{\partial}{\partial n'}\,g_2(\boldsymbol{r},\boldsymbol{r}')\,\mathrm{d}\,\ell', \quad z \geq h, \tag{4c}$$

where v_0 is the mean value of exciting potential $V_1(\boldsymbol{r})$ on the boundary contour L:

$$v_0 = \frac{1}{|L|}\int\limits_L V_1(\boldsymbol{r})\,\mathrm{d}\,\ell. \tag{5}$$

In the formulae (4a–c) the calculation point $P(\boldsymbol{r}) \equiv (x, z)$ lies outside L. The point $Q(\boldsymbol{r}') \equiv (x', z')$ lies on the contour L; it is the running integration point. The function $f(\boldsymbol{r})$ occurring in (4a–c) is a modified double layer density distributed along curve L which is simply related to the potential $U_T(\boldsymbol{r})$ on L:

$$f(\boldsymbol{r}) = (1 - \lambda_T/\lambda_1)[U_T(\boldsymbol{r}) - v_0], \qquad P(\boldsymbol{r}) \in L. \tag{6}$$

This density must be calculated by means of the boundary integral equation (B.I.E.):

$$f(\boldsymbol{r}) = 2\beta\,[V_1(\boldsymbol{r}) - v_0] + \frac{\beta}{\pi}\,⨍\limits_L f(\boldsymbol{r}')\frac{\partial}{\partial n'}g_1(\boldsymbol{r},\boldsymbol{r}')\,\mathrm{d}\,\ell',$$

$$\beta = (1 - \lambda_T/\lambda_1)/(1 + \lambda_T/\lambda_1), \qquad P(\boldsymbol{r}) \in L. \tag{7}$$

The back slash in the integral sign in (7) denotes integration in the principal value sense.

2. Greens functions of our geothermal problem

The formulae given above, involve the normal derivatives of Green's functions $g_1(\boldsymbol{r}, \boldsymbol{r}')$, $g_2(\boldsymbol{r}, \boldsymbol{r}')$. In what follows, the basic singular part in these functions is logarithm of expression $|\boldsymbol{r} - \boldsymbol{r}'|^{-1} = [(x - x')^2 + (z - z')^2]^{-1/2}$. Its normal derivative is calculated by means of formula:

$$\frac{\partial}{\partial n'} \ln |\boldsymbol{r} - \boldsymbol{r}'|^{-1} = \frac{\boldsymbol{n}' \cdot (\boldsymbol{r} - \boldsymbol{r}')}{|\boldsymbol{r} - \boldsymbol{r}'|^2} = \frac{n'_x(x - x') + n'_z(z - z')}{|\boldsymbol{r} - \boldsymbol{r}'|^2}, \tag{8}$$

where $\boldsymbol{n}' \equiv (n'_x, n'_z)$ is the outer normal vector to the contour line L, which is in our case composed of N segments T_k. These functions obey the following two-dimensional equations:

$$\nabla^2 g_1(\boldsymbol{r}, \boldsymbol{r}') = -2\pi\delta(x - x')\delta(z - z'), \tag{9}$$

$$\nabla^2 g_2(\boldsymbol{r}, \boldsymbol{r}') = 0, \tag{10}$$

where $\nabla^2 \equiv \partial^2/\partial x^2 + \partial^2/\partial z^2$ is 2D Laplace operator. The boundary conditions on planes $z = 0$ and $z = h$ are:

$$g_1|_{z=0} = 0, \tag{11}$$

$$g_1|_{z=h} = g_2|_{z=h}\,, \tag{12}$$

$$[\partial g_1/\partial z]_{z=h} = (\lambda_2/\lambda_1)\,[\partial g_2/\partial z]_{z=h}\,. \tag{13}$$

On the right side of the Poisson equation (9) we have the two-dimensional Dirac's function $\delta(\boldsymbol{r} - \boldsymbol{r}') = \delta(x - x')\delta(z - z')$, with the singularity in points (x', z') lying on the boundary line L of the perturbing body. The theory of the classical potential shows that this singularity holds true for potential of y-directed line source:

$$\ln |\boldsymbol{r} - \boldsymbol{r}'|^{-1} = \ln \left[(x - x')^2 + (z - z')^2\right]^{-1/2}, \tag{14}$$

as a fundamental solution of 2D Poisson equation

$$\nabla^2 \ln |\boldsymbol{r} - \boldsymbol{r}'|^{-1} = -2\pi\delta(\boldsymbol{r} - \boldsymbol{r}'). \tag{15}$$

This logarithmic potential represents the basic part of $g_1(\boldsymbol{r}, \boldsymbol{r}')$. Moreover it must contain some harmonic part in order to satisfy the boundary conditions (12), (13). Using the knowledge from 3D geothermal problem *(Hvoždara and Valkovič, 1999)* we have 2D analogs of Green's function of the form:

$$\begin{aligned} g_1(\boldsymbol{r}, \boldsymbol{r}') = & \ln\left[\eta^2 + (z-z')^2\right]^{-1/2} - \ln\left[\eta^2 + (z+z')^2\right]^{-1/2} - \\ & - \sum_{n=1}^{\infty} \kappa^n \left\{ \ln\left[\eta^2 + (2nh - z - z')^2\right]^{-1/2} - \right. \\ & \left. - \ln\left[\eta^2 + (2nh - z + z')^2\right]^{-1/2} \right\} - \\ & - \kappa^n \left\{ \ln\left[\eta^2 + (2nh + z - z')^2\right]^{-1/2} - \right. \\ & \left. - \ln\left[\eta^2 + (2nh + z + z')^2\right]^{-1/2} \right\}, \end{aligned} \tag{16}$$

$$\begin{aligned} g_2(\boldsymbol{r}, \boldsymbol{r}') = (1-\kappa) \Bigg\{ & \ln\left[\eta^2 + (z-z')^2\right]^{-1/2} - \ln\left[\eta^2 + (z+z')^2\right]^{-1/2} - \\ & - \sum_{n=1}^{\infty} \kappa^n \left\{ \ln\left[\eta^2 + (2nh + z - z')^2\right]^{-1/2} - \right. \\ & \left. - \ln\left[\eta^2 + (2nh + z + z')^2\right]^{-1/2} \right\} \Bigg\}, \end{aligned} \tag{17}$$

where $\eta^2 = (x - x')^2$ and $\kappa = (1 - \lambda_1/\lambda_2)/(1 + \lambda_1/\lambda_2)$. Now we have prepared the Green's functions as kernels of integral solution expressed by (4a–c). These Green's functions contain harmonic parts as well, they take the form of infinite series. We note that $g_1(\boldsymbol{r}, \boldsymbol{r}')$ can contain another singularity caused by the term $-\kappa \ln\left[\eta^2 + (2nh - z - z')^2\right]^{-1/2}$ if $n = 1$ and both $z \to h$, $z' \to h$, i.e. the body touches the bottom planar boundary $z = h$. Let us denote by L_h the part of L which touches the bottom boundary $z = h$. Then this singularity can be treated similarly as $\ln|\boldsymbol{r} - \boldsymbol{r}'|^{-1}$ with some modifications to $-\kappa \ln\left[\eta^2 + (\zeta - z')^2\right]^{-1/2}$, where $\zeta = 2h - z$. Similar situation occurs if the body touches the boundary $z = 0$ by some segment L_0. Then for this segment we must treat as singular not only the term $\ln|\boldsymbol{r} - \boldsymbol{r}'|^{-1}$, but also the term $\ln\left[\eta^2 + (z + z')^2\right]^{-1/2}$. The careful treatment of these "contact cases", similarly as was performed in *Hvoždara and Valkovič (1999)* for the 3D body, gives the modified boundary integral equation in place of (7):

$$f(\boldsymbol{r}) = 2\gamma(P)\left[V_1(\boldsymbol{r}) - v_0\right] + \frac{\gamma(P)}{\pi} \oint_L f(\boldsymbol{r}') \frac{\partial}{\partial n'} g_1(\boldsymbol{r}, \boldsymbol{r}')\, \mathrm{d}\,\ell', \tag{18}$$

where $\gamma(P)$ is the discontinuous coefficient of the integral equation

$$\gamma(P) = \left| \begin{array}{l} \beta = (1-\lambda_T/\lambda_1)/(1+\lambda_T/\lambda_1), \text{ for } P \notin L_h, \quad P \notin L_0, \\ \beta_h = \beta/(1+\kappa\beta), \text{ for } P \in L_h, \\ \beta_0 = (1-\lambda_T/\lambda_1)/2, \text{ for } P \in L_0. \end{array} \right. \tag{19}$$

This enhancement for contact cases enables us to calculate more interesting model bodies useful for practice.

3. Algorithm for numerical calculations

In the numerical calculations we can use most of the experience from solutions of the B.I.E. in the simpler case *(Hvoždara, 1983, 1986)*, where the Green's function is only of the form $\ln|\boldsymbol{r}-\boldsymbol{r}'|^{-1}$ as well as in the mathematically similar magnetometric problem considered in *Hvoždara and Kaplíková (2005)*. The key for numerical solution of the B.I.E. is necessity to have formulae for the normal derivatives of both terms in $g_1(\boldsymbol{r}, \boldsymbol{r}')$ given by (16). For the first part we have the expression given by (9) and we need to integrate it along elementary segments Δs_ℓ, which in the collocation method of solution of B.I.E. compose the whole contour L. According to explanation given in *Hvoždara (1983)*, for the integral of the principal logarithmic term in both $g_1(\boldsymbol{r}, \boldsymbol{r}')$ and $g_2(\boldsymbol{r}, \boldsymbol{r}')$ we have

$$\int_{\Delta s_\ell} \frac{\partial}{\partial n'} \ln\left[(x-x')^2 + (z-z')^2\right]^{-1/2} \mathrm{d}\,\ell' = \int_{\Delta s_\ell} \frac{\boldsymbol{n}' \cdot (\boldsymbol{r}-\boldsymbol{r}')}{|\boldsymbol{r}-\boldsymbol{r}'|^2}\, \mathrm{d}\,\ell' = $$
$$= \omega(P_j, Q_\ell), \tag{20}$$

where $\omega(P_j, Q_\ell)$ is the plane angle of the view subtended from the point P_j onto segment Δs_ℓ with the central point Q_ℓ and outer normal $\boldsymbol{n}'$, while this angle must be multiplied by the signum of the scalar product of vectors $\boldsymbol{n}'$ and $(\boldsymbol{r}-\boldsymbol{r}')$. By means of the cosine theorem applied to the triangle scheme in Fig. 2 we obtain

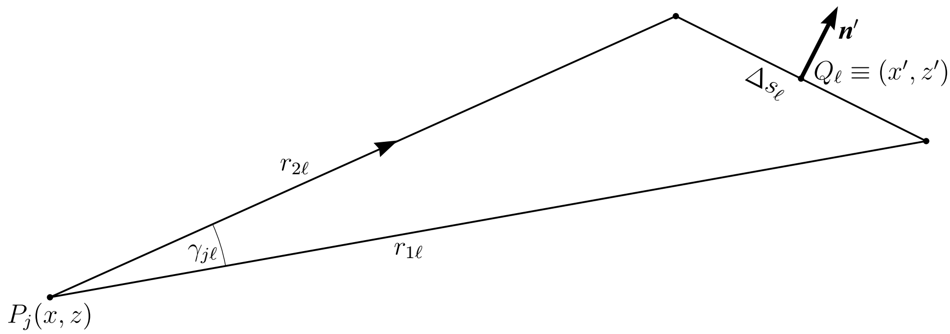

Fig. 2. Explanation sketch to the calculation of the plane angle of view onto a linear segment.

$$\Delta s_\ell = \left[r_{1\ell}^2 + r_{2\ell}^2 - 2\, r_{1\ell}\, r_{2\ell} \cos\gamma_{j\ell}\right]^{1/2},$$

so the value of cosine for $\gamma_{j\ell}$ is

$$\cos\gamma_{j\ell} = \left[r_{1\ell}^2 + r_{2\ell}^2 - (\Delta s_\ell)^2\right] / 2 r_{1\ell} r_{2\ell}, \tag{21}$$

and for $\omega(P_j, Q_\ell)$ we have:

$$\omega(P_j, Q_\ell) = \gamma_{j\ell}\, \mathrm{sign}\left[\boldsymbol{n}' \cdot (\boldsymbol{r}-\boldsymbol{r}')\right]. \tag{22}$$

For the normal derivative of the second logarithmic part in $g_1(\boldsymbol{r}, \boldsymbol{r}')$ we use similar reasoning, so we can write

$$\omega^*(P_j^*, Q_\ell) = \int\limits_{\Delta s_\ell} \frac{\boldsymbol{n}' \cdot (\boldsymbol{r}_{*j} - \boldsymbol{r}')}{|\boldsymbol{r}_{*j} - \boldsymbol{r}'|^2}\, \mathrm{d}\,\ell' = \int\limits_{\Delta s_\ell} \frac{n'_x(x_j - x') + n'_z(-z_j - z')}{(x_j - x')^2 + (z_j + z')^2}\, \mathrm{d}\,\ell' =$$
$$= \gamma_{j\ell}^* \cdot \mathrm{sign}\left[\boldsymbol{n}'(\boldsymbol{r}_* - \boldsymbol{r}')\right]. \tag{23}$$

The geometrical sense of the angle $\gamma_{j\ell}^*$ is identical with the plane angle of view from the point $P^* \equiv (x, -z)$ onto segment Δs_ℓ around the point $Q_\ell \in L$. As mentioned above, for the collocation solution of the B.I.E.

we divide each segment T_k into smaller pieces of equal length Δs_ℓ, their number being m_k and the sum of m_k equal to M. For practical use we suggest $5 \le m_k \le 20$, according to the length T_k. So we must keep

$$\sum_{k=1}^{N} m_k = M, \tag{24}$$

where the total number M of segments Δs_ℓ should be 50–100 according to the total length L. The numbers m_k must be optional for purposes of the accuracy tests of solution of the B.I.E. (7). As we already mentioned, this method assumes the piecewise constant approximation of the unknown function $f(P)$ - its value is equal to the centred one $f(Q_\ell)$ in the whole segment $\Delta\ell_j$. Then we can write the B.I.E. (7) in the form

$$f(P_j) = 2\beta\,[V_1(P_j) - v_0] + \frac{\beta}{\pi}\sum_{\ell=1}^{M}{}^{*} f(Q_\ell)\,u(P_j, Q_\ell), \tag{25}$$

where asterisk over the summation sign denotes omission of the contribution from $\ln|\boldsymbol{r}-\boldsymbol{r}'|^{-1}$ on the segment Δs_ℓ, where $P_j \equiv Q_\ell$, in accordance with the rules of principal value integration. From the explanation by the formula (20) follows that in this situation the normal vector $\boldsymbol{n}'$ is perpendicular to the vector $(\boldsymbol{r}_j - \boldsymbol{r}')$ for the points $Q(\boldsymbol{r}') \in T_k$, $P(\boldsymbol{r}) \in T_k$, which simplifies numerical calculations since the singular terms do not arise.

The weighting factors $u(P_j, Q_\ell)$ in (25) have the integral forms as:

$$u(P_j, Q_\ell) = \int\limits_{\Delta s_\ell} \frac{\partial}{\partial n'} g_1(\boldsymbol{r}, \boldsymbol{r}')\,\mathrm{d}\,\ell', \tag{26}$$

which involve both angles of view $\gamma_{j\ell}$, $\gamma^*_{j\ell}$ onto segment Δs_ℓ and also contribution due to all terms of the infinite series in $g_1(\boldsymbol{r}, \boldsymbol{r}')$. The equation (25) tells us that into value $f(P_j)$ there are incorporated contributions from all $f(Q_\ell)$ (with some weighting factors) at segments Δs_ℓ forming L.

The geometrical relations occurring in numerical calculations are illustrated with the example of segment T_3 depicted in Fig. 3, similarly as in *Hvoždara and Kaplíková (2005).* This segment connects the points A_3 and A_4 creating 6 subsegments (pieces) with centres $Q_{3,0} - Q_{3,5}$. The normal vector for the whole segment T_3 is $\boldsymbol{n}'_3$ and its Carthesian components calculated from equations $\boldsymbol{n}'_3 \times \boldsymbol{T}_3/T_3 = \mathbf{1}$ and $\boldsymbol{n}'_3 \cdot \boldsymbol{T}_3 = 0$, which reflects mutual

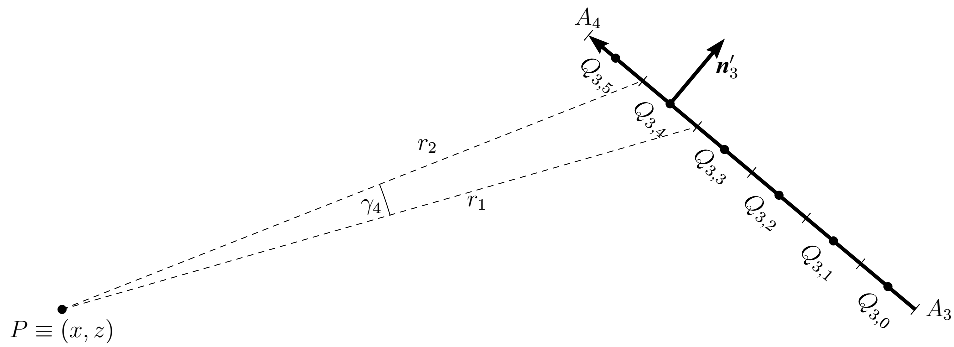

Fig. 3. Subdivision of the vector T_3 into six subsegments.

orthogonality of vectors $\boldsymbol{T}_3$ and $\boldsymbol{n}'_3$. Then it is clear that $\boldsymbol{n}'_3$ is constant unit vector for the whole segment T_3, its components can be calculated from coordinates of terminal points A_3, A_4. The length of the vector $\boldsymbol{T}_3 = \boldsymbol{A}_3\boldsymbol{A}_4$ is given by the formula (1):

$$T_3 = \left[(x'_4 - x'_3)^2 + (z'_4 - z'_3)^2\right]^{1/2}, \tag{27}$$

because the vector $\boldsymbol{T}_3$ is:

$$\boldsymbol{T}_3 = (x'_4 - x'_3)\boldsymbol{e}_x + (z'_4 - z'_3)\boldsymbol{e}_z. \tag{28}$$

As we already noted the relations: $\boldsymbol{n}'_3 \times \boldsymbol{T}_3/T_3 = \boldsymbol{1}$ and $\boldsymbol{n}'_3 \cdot \boldsymbol{T}_3 = 0$, have to be fulfilled since the angle between $\boldsymbol{n}'_3$ and $\boldsymbol{T}_3$ is $\pi/2$. Then we can easily find the carthesian components of $\boldsymbol{n}'_3$:

$$n'_x = -\frac{z'_4 - z'_3}{T_3}, \qquad n'_z = +\frac{x'_4 - x'_3}{T_3}. \tag{29}$$

We apply similar treatment for all vector segments $\boldsymbol{T}_k$. We see that as soon as we have defined contour polygon L of the perturbing body, we can easily determine normal vectors $\boldsymbol{n}'$ on all vector segments $\boldsymbol{T}_k$. These values must be used for calculations of weighting factors for discretized B.I.E. From treatment given in *Hvoždara (1983)* we know that the term $\omega(P_j, Q_\ell) = \gamma_{\ell j}\,\mathrm{sign}\,[\boldsymbol{n}'_\ell \cdot (\boldsymbol{r}_j - \boldsymbol{r}'_\ell)]$ is the most important term in the weighting factor $u(P_j, Q_\ell)$. For the case of convex contour line L as shown in Fig. 1 all these values will be negative or zero, because $\mathrm{sign}[\boldsymbol{n}'_\ell \cdot (\boldsymbol{r}'_j - \boldsymbol{r}'_\ell)] < 0$, since the angles between $\boldsymbol{n}'_\ell$ and $(\boldsymbol{r}'_j - \boldsymbol{r}'_\ell)$ are obtuse. The zero value is obtained for the case when $P(\boldsymbol{r}_j)$ and $Q(\boldsymbol{r}_\ell)$ belong to the same straight line segment. It is also necessary to note that for the contour integral of the plane angle of view the very important formula – the Gaussian integral *(Tichonov and Samarskij, 1966)* holds true:

$$\oint\limits_L \frac{\boldsymbol{n}' \cdot (\boldsymbol{r} - \boldsymbol{r}')}{|\boldsymbol{r} - \boldsymbol{r}'|^2} \,\mathrm{d}\,\ell' = \begin{cases} 0, \text{ for } P(\boldsymbol{r}) \in \mathrm{Ext}(L) \\ -\pi, \text{ for } P(\boldsymbol{r}) \in L \\ -2\pi, \text{ for } P(\boldsymbol{r}) \in \mathrm{Int}(L)\,. \end{cases} \tag{30}$$

The case $P(\boldsymbol{r}) \in L$ of this formula provides us with very good check of accuracy of calculation of $\omega(P_j, Q_\ell)$, because at the calculation of the weighting factors of the B.I.E. (7) we have to fulfill the control value:

$$\sum_{\ell=1}^{M} \omega(P_j, Q_\ell) \doteq -\pi \tag{31}$$

with accuracy better than 1%, otherwise we did not introduce fine enough subdivision of the contour L, or in our program code we have another errors. The second term in $g_1(\boldsymbol{r} - \boldsymbol{r}')$ is the function $\ln|\boldsymbol{r}_* - \boldsymbol{r}'|^{-1}$ which is harmonic and from the Gaussian integral (30) its check value follows:

$$\sum_{\ell=1}^{M} \omega^*(P_j^*, Q_\ell) \doteq 0, \tag{32}$$

because for $\ln|\boldsymbol{r}_* - \boldsymbol{r}'|^{-1}$ the point of view $P^* \equiv (x, -z)$ lies in $\mathrm{Ext}(L)$. Similar property (zero value) must be obtained also for contributions due to terms of the infinite series in Green's function $g_1(\boldsymbol{r}, \boldsymbol{r}')$. The discretized form of B.I.E. (7) can be written as a classical system of M linear equations:

$$\sum_{\ell=1}^{M} C_{\ell j} X_\ell = b_j, \quad j = 1, 2, \ldots, M, \tag{33}$$

$$\text{where} \quad b_j = 2\beta[V_1(P_j) - v_0], \tag{34}$$

are elements of the right side vector (they represent values of the exciting potentials) on elements $\Delta\ell_j$. The elements of the matrix of the system (33) are

$$C_{\ell j} = \delta_{\ell j} - \beta\pi^{-1}u(P_j, Q_\ell), \tag{35}$$

where $\delta_{\ell j}$ is the Kronecker's symbol ($\delta_{\ell j} = 1$ if $\ell = j$ and $\delta_{\ell j} = 0$ for $\ell \neq j$). Values of (as yet) unknown function $f(Q)$ collocated for centres of intervals Δs_ℓ are represented in elements of solution vector $X_\ell = f(Q_\ell)$. The system of Eq. (33) expresses that contributions from all M elements of the contour polygon are included in each value $f(Q_j)$. It is necessary to stress that the subdivision to elements Δs_ℓ must be dense enough, because the theory of potential requires continuity of $f(Q)$ along L, which means that the changes of neighbouring values $f(Q_\ell)$ should not be greater than 5–10%. If this condition of "quasi continuity" is not satisfied on some segment T_k we must increase the number of subdivision. Another check of accuracy is based on comparison of values $f(Q_\ell)$ for gradually increased number of subdivision (M), e.g. M = 50, 80, 120, 160 which is easily possible to perform on contemporary PC-computers. As soon as the solution of (33) is performed with satisfactory accuracy, we can calculate approximations of temperatures U_1 or U_2, U_T by means of formulae (4a–c). From the practical viewpoint the values of the heat flow density, especially of its vertical anomalous part are also of interest.

4. Calculations of the temperature and heat flow anomalies

The unperturbed temperature $V_1(z)$ in the upper layer is characterized by the linear formula (2) and the corresponding normal geothermal heat flow is uniform inside the layer "1":

$$q_0 = +\lambda_1 \partial V_1/\partial z. \tag{36}$$

We note that we are using geophysical convention for the z-component for the heat flow density calculation – i.e. positive derivation with respect to the z-coordinate pointing vertically downward into the earth (the physically correct definition $\boldsymbol{q} = -\lambda \operatorname{grad} U$ would cause that the q_z values are negative almost everywhere since the temperature $U(x,z)$ as a rule increases with depth z). The anomalous vertical heat flow in the layer "1" of our model is:

$$\Delta q = \lambda_1 \partial(\Delta T)/\partial z, \tag{37}$$

where ΔT is the temperature anomaly in the first layer:

$\Delta T = U_1 - V_1.$

According to the applied collocation method, we have the approximation:

$$\Delta T(P) = \frac{1}{2\pi} \sum_{\ell=1}^{M} f(Q_\ell) u(P, Q_\ell), \quad P \in \mathrm{Ext}(L), \tag{38}$$

where $P(x, z)$ is the point of calculation outside the perturbing body and $u(P, Q_\ell)$ are weighting factors:

$$u(P, Q_\ell) = \int\limits_{\Delta s_\ell} \frac{g_1(P, Q)}{\partial n'} \, \mathrm{d}\, \ell_Q. \tag{39}$$

Following the important checking properties (30) we must achieve with high accuracy (about 0.001) the test value:

$$\sum_{\ell=1}^{M} u(P, Q_\ell) = 0, \tag{40}$$

since the point of view $P \in \mathrm{Ext}(L)$. The region above the perturbing body is the most interesting region for numerical calculation, i.e. for $z \in \langle 0, h_T \rangle$ where $h_T = (z_u + z_b)/2$ is the depth of the central plane of the perturbing body, while z_u, z_b are z-coordinates of the upper or bottom boundary of the body. We choose few levels z_k in the interval $\langle 0, h_T \rangle$ and calculate anomalous temperatures for two shifted levels around z_k, i.e. $\Delta T(x, z_k - \epsilon)$ and $\Delta T(x, z_k + \epsilon)$ along x-profile points $x \in \langle -L, +L \rangle$ well covering the horizontal width of the perturbing body. Then we calculate the approximation of the vertical heat flow anomaly

$$\Delta q(x, z_k) = \lambda_1 \left[\Delta T(x, z_k + \epsilon) - \Delta T(x, z_k - \epsilon) \right] / (2\epsilon), \tag{41}$$

where ϵ is small increment of z_k, e.g. $\epsilon = z_u/20$.

In Fig. 4a we present the results of numerical calculations for the body of rectangle cross-section having $\lambda_T/\lambda_1 = 2$ and the top boundary in the depth $z_u = 0.5$ m, while for the Fig. 4b we take $z_u = 0.2$ m. In both cases there is also $\lambda_2 = \lambda_T$ and the bottom boundary z_b is at the depth $z_b = 2.5$ m ($= h \equiv h_v$), so the prism represents intrusion of the substratum into first

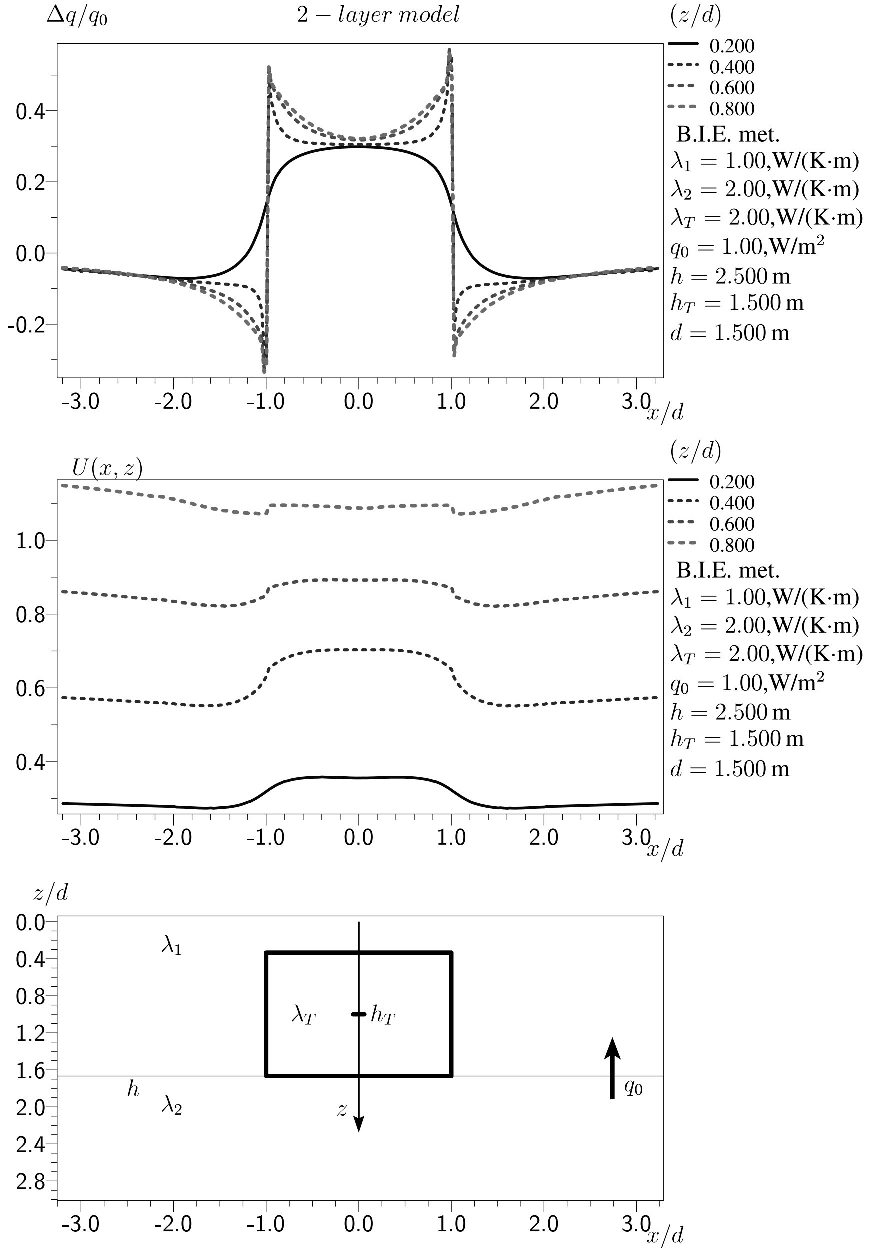

Fig. 4a. Anomalies of $\Delta q/q_0$ and temperatures $U(x,z)$ at four levels z/d above the rectangular 2D prism with $\lambda_T/\lambda_1 = 2$, $z_u = 0.5\,\mathrm{m}$, $z_b = 2.5\,\mathrm{m}$.

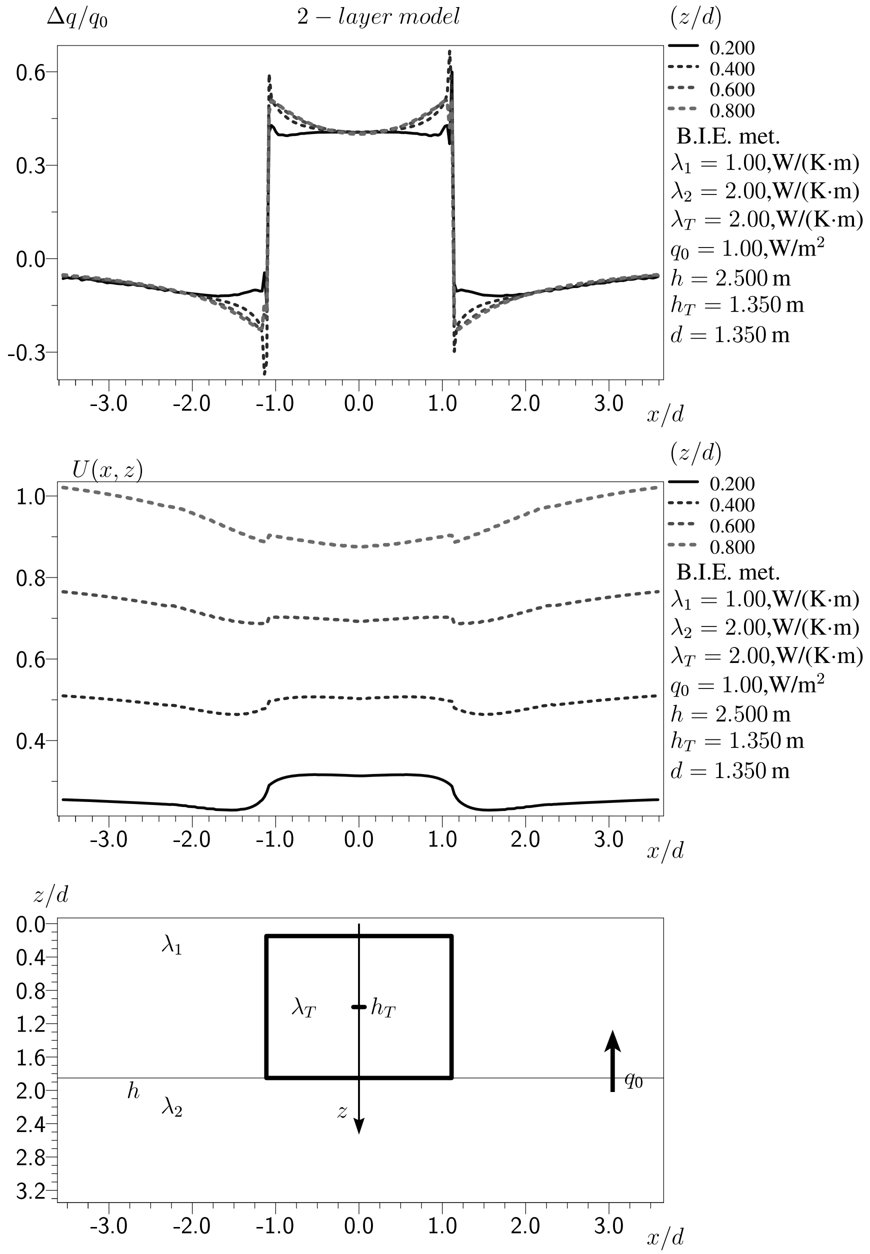

Fig. 4b. The same as in Fig. 4a, but for $z_u = 0.2\,\mathrm{m}$.

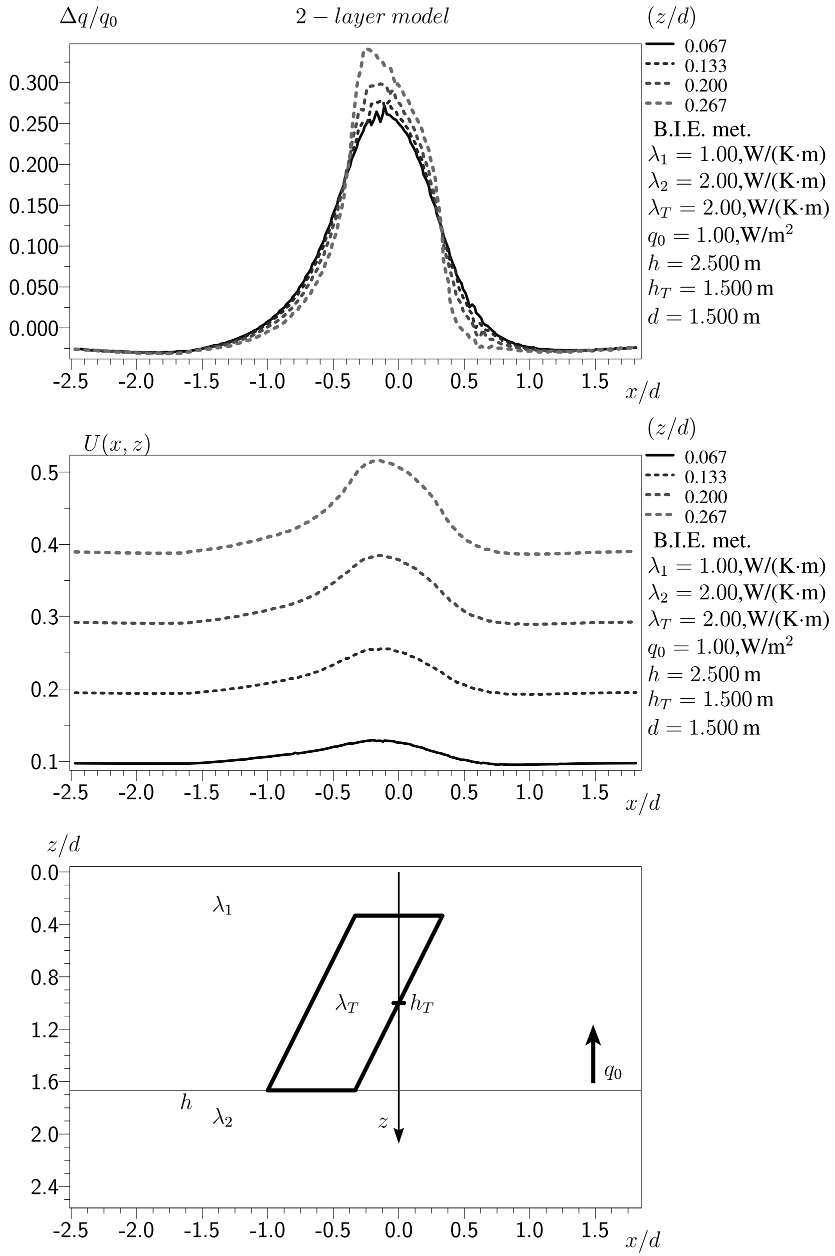

Fig. 5a. Anomalies of $\Delta q/q_0$ and temperature $U(x,z)$ at four levels z/d above the 2D prism of trapezoidal cross-section with $\lambda_T/\lambda_1 = 2$, $z_u = 0.5$ m, $z_b = 2.5$ m.

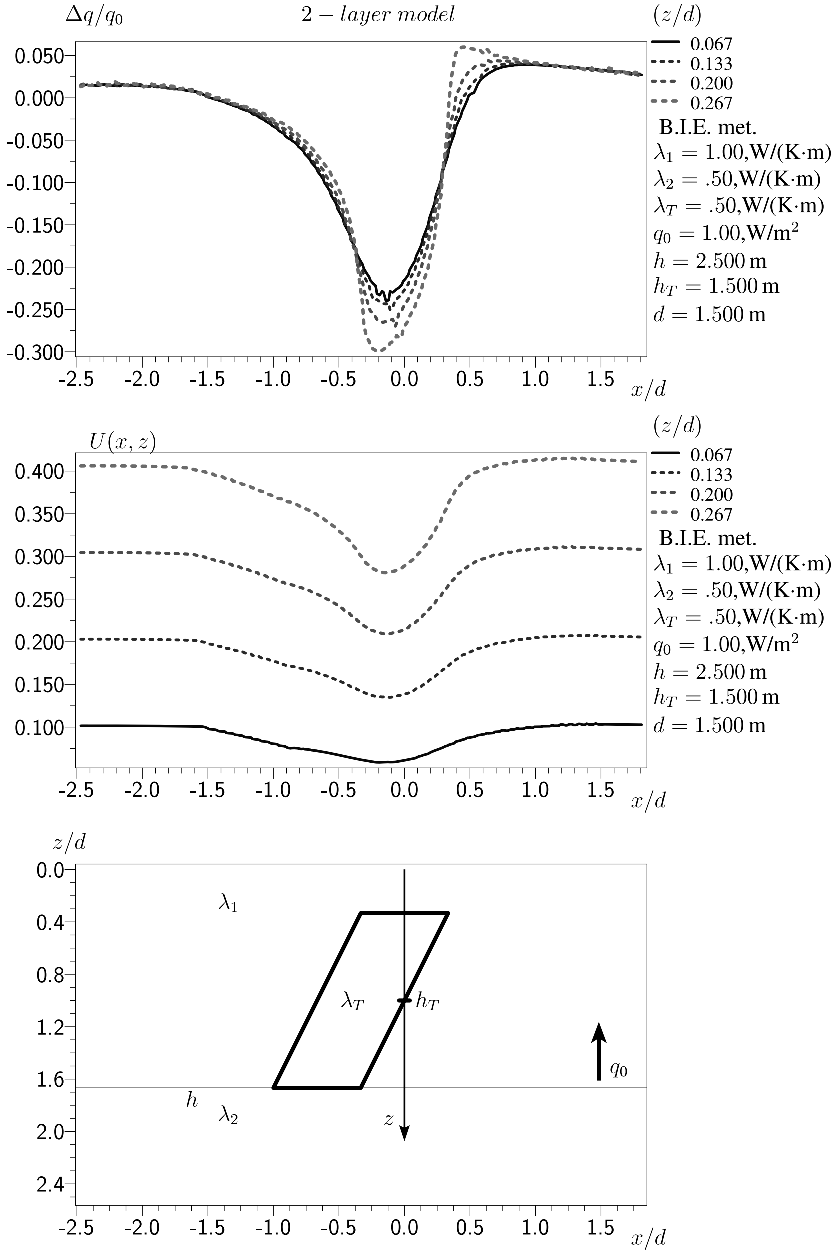

Fig. 5b. The same as in Fig. 5a but for $\lambda_T/\lambda_1 = 0.5$.

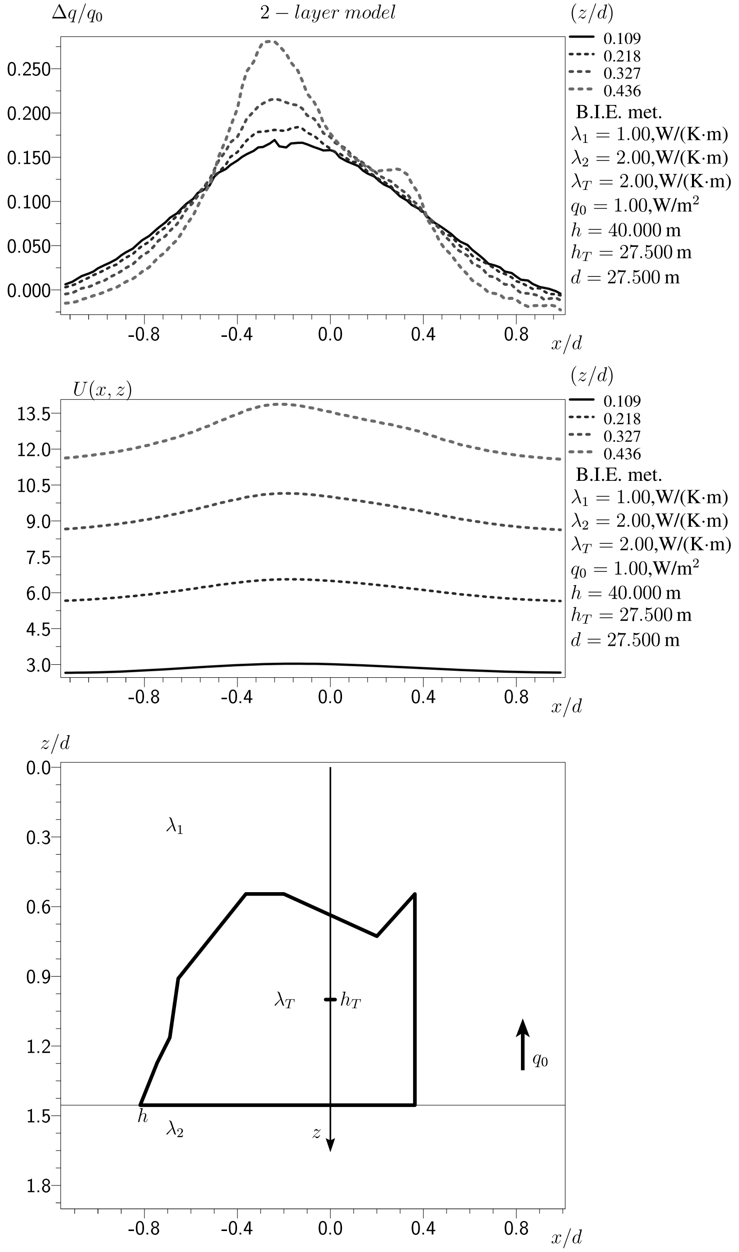

Fig. 6a. Anomalies of $\Delta q/q_0$ and temperature $U(x,z)$ at four levels z/d above the 2D prism of polygonal cross-section with $\lambda_T/\lambda_1 = 2$.

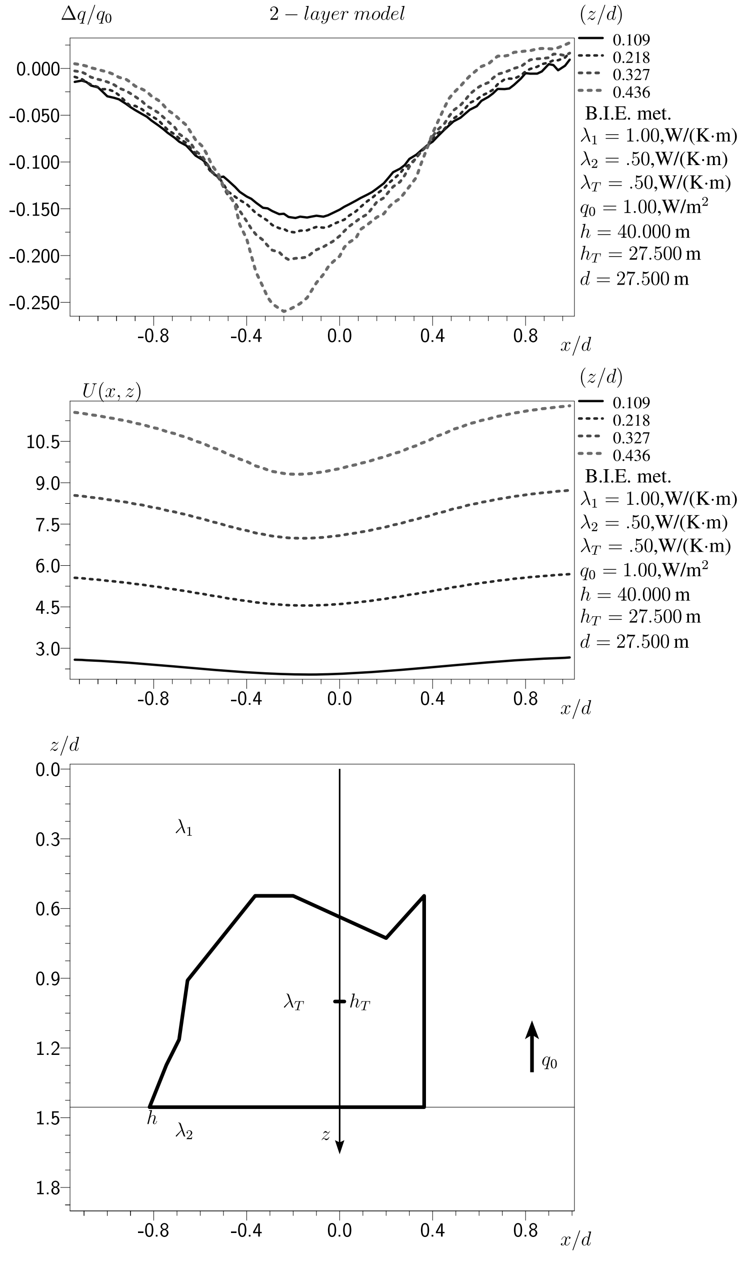

Fig. 6b. The same as in Fig. 6a but for $\lambda_T/\lambda_1 = 0.5$.

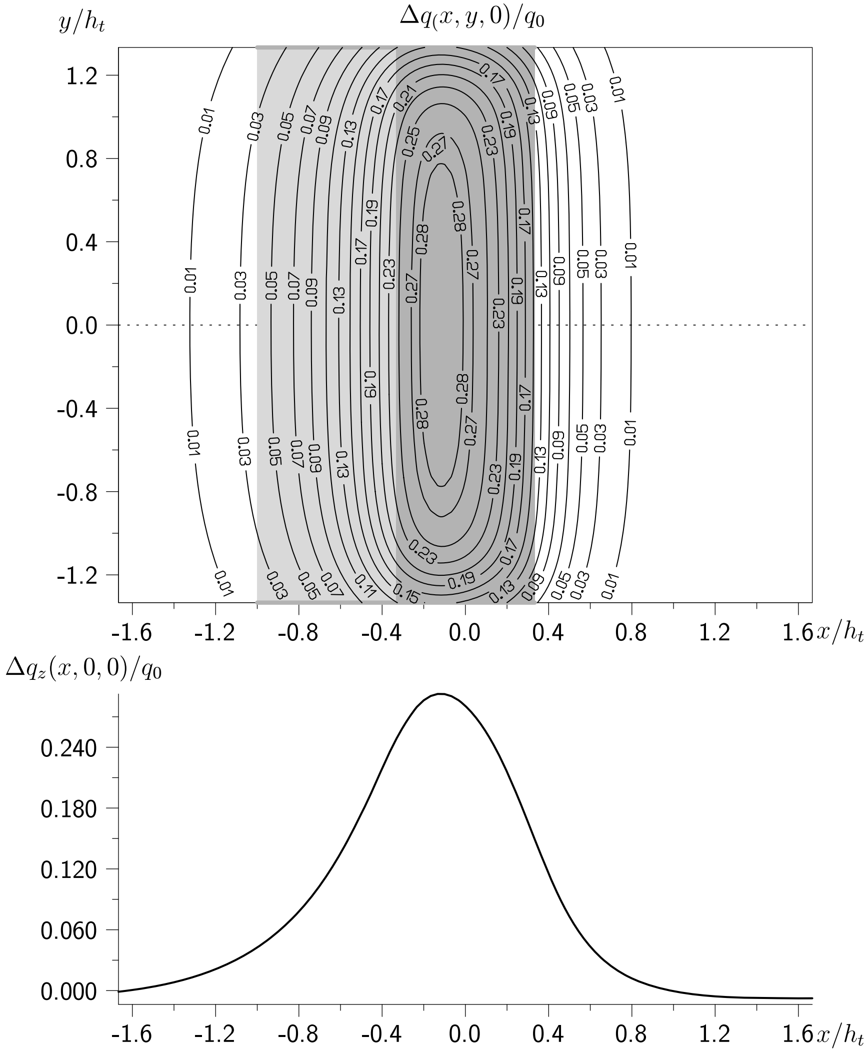

$z_1, xl, xr, yl, yr = .50$ -.50 .50 -2.00 2.00 m
$z_2, xl, xr, yl, yr = 2.50$ -1.50 -.50 -2.00 2.00 m
$h, h_t = 2.50$ 1.50 m
$\lambda_1 = 1.0$, $\lambda_2 = 2.0$, $\lambda_T = 2.00$ W/(K m)

Fig. 7a. Isolines of $\Delta q/q_0$ above the 3D prismoid elongated in y-direction and its upper rectangle shifted in x-direction. The dimensions of rectangular surfaces at z_1 (upper) and bottom at z_2 are given in table, $\lambda_T/\lambda_1 = 2$. The profile curve $\Delta q/q_0$ is plotted for $y = 0$.

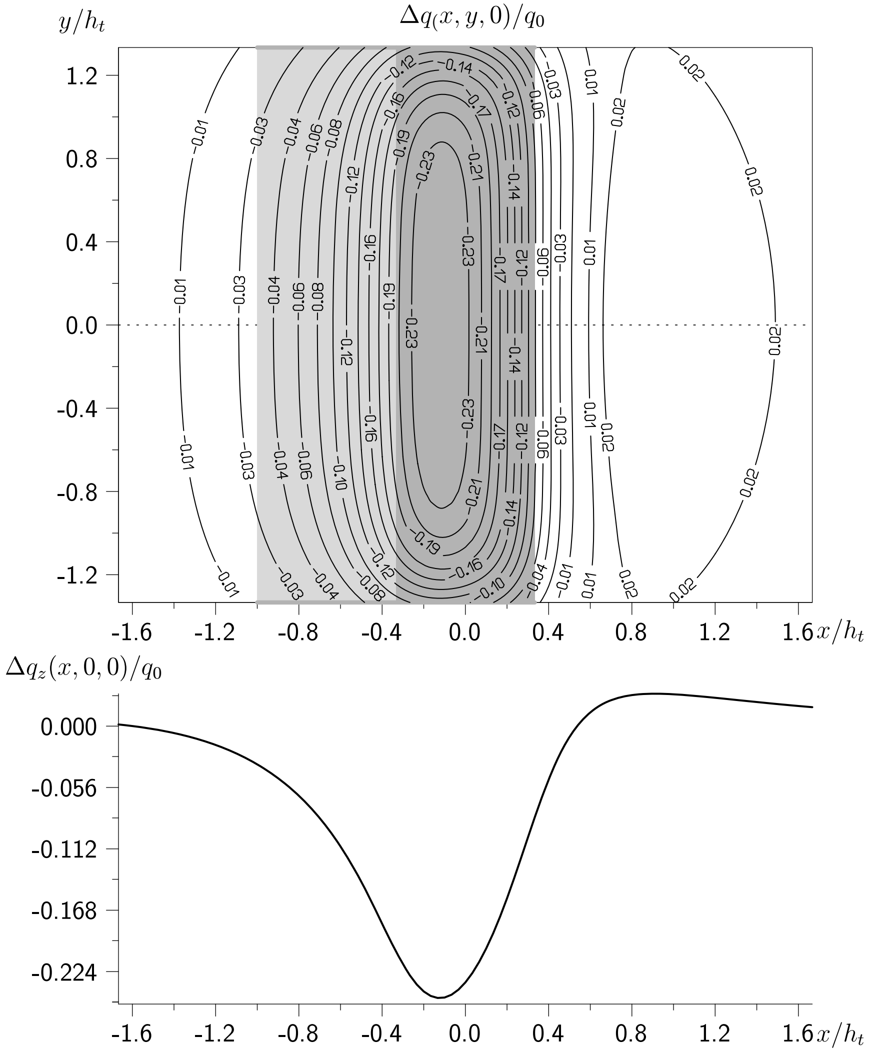

$z_1, xl, xr, yl, yr = $ .50 -.50 .50 -2.00 2.00 m
$z_2, xl, xr, yl, yr = $ 2.50 -1.50 -.50 -2.00 2.00 m
$h, h_t = $ 2.50 1.50 m
$\lambda_1 = 1.0$, $\lambda_2 = .5$, $\lambda_T = .50$ W/(K m)

Fig. 7b. The same as in Fig. 7a but for $\lambda_T/\lambda_1 = 0.5$.

layer. We can see that for $\lambda_T/\lambda_1 = 2$ we have at the surface ($z \approx 0$) about 20–40% increase of the heat flow above the prism, then the values of $\Delta q/q_0$ increase with depth z. We can see the same increase also for isotherms $U(x, z)$, plotted in the middle set of graphs. These temperatures calculated using formula (4a) if the point of calculation is outside the perturbing body and by formula (4b) for points inside of the body. We can see the steep growth of the temperature above or inside the prism. The coordinates x, z are normalized by the value $d = (z_u + z_b)/2$. The obtained graphs for $\Delta q/q_0$ are consistent with those obtained in *Hvoždara and Schlosser (1985)* where the ambient medium around rectangular prism was a halfspace.

Another interesting model body is a 2D prism with trapezoidal cross-section. The top and bottom of the body are in the same depths as for the rectangle in Fig. 4a, but its width is smaller. The curves of $\Delta q/q_0$ and $U(x, z)$ are presented in Figs 5a,b for $\lambda_T/\lambda_1 = 2$ and 0.5, respectively. We can see a slight horizontal asymmetry of anomaly curves. The anomaly in $\Delta q/q_0$ is more conspicuous in comparison to the case with rectangle cross-section. The results for the body with more complicated polygonal cross-section are presented in Figs 6a,b. In this case we can see that the topography of the upper boundary of the body is reflected in the course of $\Delta q/q_0$ for the profile at the depth $z/d = 0.436$ which is closest to the anomalous body. In all figures we can see that the temperature $U(x, z)$ is disturbed near and inside the perturbing body and far from the body it attains the levels given by the unperturbed temperature $V_1 = zq_0/\lambda_1$. It is clear that the temperature anomaly $\Delta T = U_1(x, z)$ tends to zero far from the perturbing body.

Finally, we present comparative calculations for the surface heat flow anomaly for 3D body calculated by the method presented in *Hvoždara (2008)*. This inclined 3D prism is elongated in y-direction, its upper rectangle boundary is horizontally shifted in x-direction, so its cross-section by the plane $y = 0$ is a trapezoid shown in Figs 5a,b. The results of the heat flow anomaly at the surface $z = 0$ are presented in Figs 7a,b for $\lambda_T/\lambda_1 = 2$ or 0.5, respectively. In the upper figure the isolines of the anomalous heat flow above the 3D body are plotted, and on the bottom we can see the profile curves for $y = 0$, $z = 0$. We can see that these profile curves well agree with those presented in Figs 5a,b for $\Delta q/q_0$ for the depths z/d close to zero. So we have confirmed applicability of 2D models for y-elongated bodies.

Acknowledgments. The authors are grateful to VEGA, the Slovak Grant Agency (grants: No. 2/7008/27, No. 2/0107/09) for the partial support of this work.

References

Carslaw H. S., Jaeger J. C., 1959: Conduction of heat in solids. Clarendon Press, Oxford.

Chen Y., Beck A. E., 1991: Application of the boundary element method to a terrestrial heat flow problems. Geophys. J. Int., **107**, 25–35.

Hvoždara M., 1983: Solution of the direct problem of magnetometry with the aid of the potential of a dipole layer. Contrib. Geophys. Ins. Slov. Acad. Sci., **14**, 23–46.

Hvoždara M., Schlosser G., 1985: Anomaly of the telluric and thermal field by the presence of a two-dimensional body in a homogeneous halfspace. Contrib. Geophys. Ins. Slov. Acad. Sci., **15**, 35–47.

Hvoždara M., Valkovič L., 1999: Refraction effect in geothermal heat flow due to a 3D prism in a two-layered Earth. Studia Geoph. Geod., **43**, 407–426.

Hvoždara M., Kaplíková A., 2005: Magnetometric problem for a 2D body of polygonal cross-section buried in the unbounded magnetic halfspace. Contrib. Geophys. Geod., **35**, 4, 353–372.

Hvoždara M., 2008: Refraction effect in the heat flow due to a 3D prismoid situated in a two-layered Earth. Contrib. Geophys. Geod., **38**, 4, 371–390.

Lebedev N. N., Skalskaja I. P., Ufljand Ya. S., 1955: Collection volume of problems of the mathematical physics. GITTL, Moscow (in Russian).

Ljubimova E. A., Ljuboshits V. M., Parfenjuk O. I., 1983: Numerical models of temperature fields in the Earth. Nauka, Moscow (in Russian).

Moon P., Spencer D. E., 1971: Field theory handbook, Springer-Verlag, Berlin.

Tichonov A. N., Samarskij A. A., 1966: Equations of Mathematical Physics. Nauka, Moscow (in Russian).